MIMO-Zak-OTFS in Doubly-Selective Channels: I/O Relation Estimation and Detection

Abhishek Bairwa and Ananthanarayanan Chockalingam
Department of ECE, Indian Institute of Science, Bangalore

***Abstract*—In this paper, we are concerned with Zak transform-based orthogonal time frequency space (Zak-OTFS) modulation in a multiple-input multiple-output (MIMO) setting with multiple antennas at the transmitter and receiver. We consider the problem of input-output (I/O) relation estimation and signal detection in MIMO-Zak-OTFS. Our contributions in this paper are as follows. First, we derive the system model for MIMO-Zak-OTFS. Next, we propose an I/O relation estimation scheme for MIMO-Zak-OTFS in a model-free framework. We evaluate the mean square error (MSE) performance of the proposed estimation scheme in Veh-A channel model with fractional delays and Dopplers, for different delay-Doppler (DD) pulse shaping filters, namely, sinc, Gaussian, and Gaussian-sinc filters. Gaussian filter is found to offer better MSE performance compared to sinc and Gaussian-sinc filters, because of the very low side lobes in Gaussian filter. Further, we assess the MIMO-Zak-OTFS signal detection performance using the estimated I/O relation. In this, Gaussian-sinc filter is found to achieve better bit error rate (BER) performance because of the good balancing characteristics of its main lobe and side lobes. We also show that a low-complexity local search based algorithm improves the minimum mean square error (MMSE) detection performance of MIMO-Zak-OTFS.**

***Index Terms*—Zak-OTFS, MIMO, delay-Doppler domain, pulse shaping, I/O relation estimation, signal detection.**

I. Introduction

High-mobility scenarios and higher frequency bands of operation are expected to be prominent in next generation wireless communication systems, resulting in large Doppler spreads of the channel. For such highly time-selective channels, current multicarrier based modulation schemes are found to be inadequate. Orthogonal time frequency space (OTFS) modulation, a delay-Doppler (DD) domain modulation, has been shown to offer robust performance in doubly-selective channels [1]-[5]. In OTFS, information symbols are multiplexed in the DD domain and transformed to time domain for transmission. In multicarrier OTFS (MC-OTFS) [1]-[5], this transformation is carried out in two steps, viz., inverse symplectic finite Fourier transform for DD domain to time-frequency (TF) domain conversion followed by Heisenberg transform for TF domain to time domain conversion. In Zak transform-based OTFS (Zak-OTFS) [6]-[10], the DD domain to time domain conversion is carried out in a single step using inverse Zak transform. Compared to MC-OTFS, Zak-OTFS has been shown to be more resilient over a larger delay and Doppler spreads [7],[8].

This work was supported in part by the J. C. Bose National Fellowship, Department of Science and Technology, Government of India.

The basic information carrier in Zak-OTFS is a quasi-periodic DD pulse [6]-[8]. A DD domain pulse shaping filter is used at the transmitter to limit the bandwidth and time duration of transmission. Commonly used pulse shaping filters include sinc, root raised cosine, Gaussian, and Gaussian-filters [7]-[15]. Input-output relation estimation and signal detection are two important tasks at the Zak-OTFS receiver. In the Zak-OTFS literature, these receiver tasks have been considered in a single-input single-output (SISO) setting [7],[11]-[15]. For example, performing I/O relation estimation task using model-dependent and model-free approaches have been considered [7],[11],[12],[15]. Likewise, the signal detection task using minimum mean square error (MMSE) based and local neighborhood search based approaches have been considered [7],[11],[12],[14],[15]. Zak-OTFS I/O relation estimation and signal detection in a MIMO setting has not been reported, which remains the focus of this paper. Our contributions in this paper can be summarized as follows.

- First, we derive the system model for MIMO-Zak-OTFS.
- Next, we propose an I/O relation estimation scheme for MIMO-Zak-OTFS in a model-free framework. We evaluate the mean square error (MSE) performance of the proposed estimation scheme in the vehicular-A (Veh-A) channel model with fractional delays and Dopplers [17], for different DD pulse shaping filters, namely, sinc, Gaussian, and Gaussian-sinc filters. Gaussian filter is found to offer better MSE performance compared to sinc and Gaussian-sinc filters, because of the very low side lobes in Gaussian filter.
- Further, we assess the MIMO-Zak-OTFS signal detection performance using the estimated I/O relation. In this, Gaussian-sinc filter is found to achieve better bit error rate (BER) performance because of the good balancing characteristics of its main lobe and side lobes.
- We also show that a low-complexity local search based algorithm improves upon the minimum mean square error (MMSE) detection performance of MIMO-Zak-OTFS.

II. MIMO-Zak-OTFS system model

In this section, we first present the Zak-OTFS system model in a SISO setting and extend it to a MIMO setting. The block diagram of Zak-OTFS transceiver in a SISO setting is shown in Fig. 1. The basic information carrier in Zak-OTFS is a quasi-periodic DD domain pulse localized in a fundamental DD period, defined by a delay period $\tau_{\rm p}$ and a Doppler period $\nu_{\rm p}$ such that $\tau_{\rm p}\nu_{\rm p} = 1$. The fundamental DD period is defined

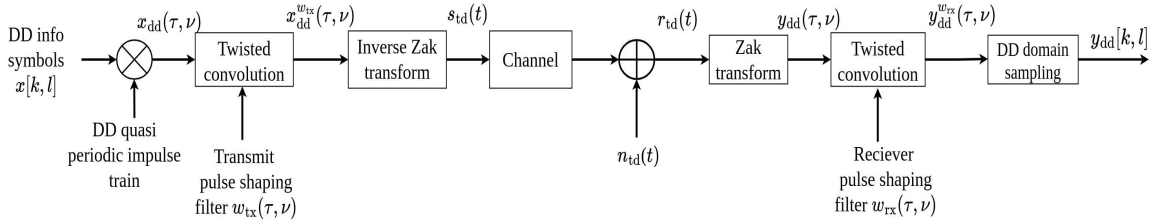

Fig. 1: Block diagram of Zak-OTFS transceiver in a SISO setting.

as $\mathcal{D}_0 = \{(\tau,\nu) \mid 0 \leq \tau < \tau_p, 0 \leq \nu < \nu_p\}$, where τ and ν represent the delay and Doppler variables, respectively, and $\tau_{\rm p}\nu_{\rm p} = 1$. A quasi-periodic DD domain pulse, when viewed in the time domain, is a pulsone which is a time domain pulse train modulated by a frequency tone. The delay period $\tau_{\rm p}$ is divided into M delay bins and the Doppler period $\nu_{\rm p}$ is divided into N Doppler bins, and MN information symbols are multiplexed on MN DD pulses located at these MN DD bins. M and N are chosen such that $MN = BT$, where B and T are the bandwidth of transmission and time duration of a Zak-OTFS frame. That is, the resolution along the delay axis is $\Delta\tau = \frac{1}{B} = \frac{\tau_{\rm p}}{M}$ and the resolution along the Doppler axis is $\Delta\nu = \frac{1}{T} = \frac{\nu_{\rm p}}{N}$. In order to limit the bandwidth and time duration to B and T, respectively, a DD domain pulse shaping filter is used at the transmitter. Figure 1 depicts the block diagram of the Zak-OTFS transceiver.

The information symbols $x[k,l]$s, $k = 0,\cdots,M-1$, $l = 0,\cdots,N-1$ are drawn from a modulation alphabet $\mathbb{A}$. The DD grid on which these MN information symbols are multiplexed is given by $\Lambda_{\rm dd} \triangleq \left\{\left(k\frac{\tau_p}{M}, l\frac{\nu_p}{N}\right) \mid k = 0,\cdots,M-1, l = 0,\cdots,N-1\right\}$. The $x[k,l]$s on $\Lambda_{\rm dd}$ are encoded as quasi-periodic discrete DD information as $x_{\rm dd}[k+nM, l+mN] = x[k,l]e^{j2\pi n\frac{l}{N}}, n,m \in \mathbb{Z}$, which is converted into a continuous DD signal by mounting on a continuous DD domain quasi-periodic impulse train, resulting in

$$x_{\rm dd}(\tau,\nu) = \sum_{k,l\in\mathbb{Z}} x_{\rm dd}[k,l]\delta\left(\tau - k\Delta\tau\right)\delta\left(\nu - l\Delta\nu\right), \quad (1)$$

where $\delta(\cdot)$ denotes Kronecker delta function. Note that $x_{\rm dd}(\tau,\nu)$ is also a quasi-periodic with period τ_p and ν_p along the delay and Doppler axes, respectively, i.e.,

$$x_{\rm dd}(\tau+n\tau_p, \nu+m\nu_p) = e^{j2\pi n\nu\tau_p}\, x_{\rm dd}(\tau,\nu),\ \forall\, n,m \in \mathbb{Z}, \quad (2)$$

The signal $x_{\rm dd}(\tau,\nu)$ is then time and bandwidth limited by filtering through the Tx DD domain filter $w_{\rm tx}(\tau,\nu)$, to obtain

$$x_{\rm dd}^{w_{\rm tx}}(\tau,\nu) = w_{\rm tx}(\tau,\nu) *_\sigma x_{\rm dd}(\tau,\nu), \quad (3)$$

where $*_\sigma$ denotes the twisted convolution[1] operation. The time domain signal for transmission is obtained using inverse Zak transform as

$$s_{\rm td}(t) = \mathcal{Z}_t^{-1}\left(x_{\rm dd}^{w_{\rm tx}}(\tau,\nu)\right) = \sqrt{\tau_p}\int_0^{\nu_p} x_{\rm dd}^{w_{\rm tx}}(t,\nu)d\nu. \quad (4)$$

[1]Twisted convolution operation between two DD functions $a(\tau,\nu)$ and $b(\tau,\nu)$ is defined as $a(\tau,\nu) *_\sigma b(\tau,\nu) = \int_{-\infty}^{\infty}\int_{-\infty}^{\infty} a(\tau',\nu')b(\tau-\tau',\nu-\nu')e^{j2\pi\nu'(\tau-\tau')}d\tau'd\nu'$. Twisted convolution operation preserves quasi-periodicity.

The transmitted signal passes through the channel having P paths whose impulse response in the DD domain is given by $h(\tau,\nu) = \sum_{i=1}^{P} h_i\delta(\tau-\tau_i)\delta(\nu-\nu_i)$, where h_i, τ_i, and ν_i are the channel gain, delay, and Doppler of the ith path, respectively. The received time domain signal is given by

$$r_{\rm td}(t) = \int\int h(\tau,\nu)s_{\rm td}(t-\tau)e^{j2\pi\nu(t-\tau)}d\tau d\nu + n(t), \quad (5)$$

where $n(t)$ is the additive white Gaussian noise (AWGN). Zak transform is used to convert the received time domain signal to DD domain as $y_{\rm dd}(\tau,\nu) = \mathcal{Z}_t(r_{\rm td}(t))$, i.e.,

$$y_{\rm dd}(\tau,\nu) = \sqrt{\tau_p}\sum_{k\in\mathbb{Z}} r_{\rm td}(\tau+k\tau_p)e^{-j2\pi\nu k\tau_p} + n_{\rm dd}(\tau,\nu), \quad (6)$$

where $n_{\rm dd}(\tau,\nu) = \mathcal{Z}_t(n(t))$ is the noise in DD domain. Next, $y_{\rm dd}(\tau,\nu)$ is filtered through the Rx DD domain filter $w_{\rm rx}(\tau,\nu)$, which is matched to the Tx DD filter, i.e., $w_{\rm rx}(\tau,\nu) = w_{\rm tx}^*(-\tau,-\nu)e^{j2\pi\tau\nu}$. The output of the Rx DD filter is given by $y_{\rm dd}^{w_{\rm rx}}(\tau,\nu) = w_{\rm rx}(\tau,\nu) *_\sigma y_{\rm dd}(\tau,\nu)$, i.e.,

$$y_{\rm dd}^{w_{\rm rx}}(\tau,\nu) = h_{\rm eff}(\tau,\nu) *_\sigma x_{\rm dd}(\tau,\nu) + n_{\rm dd}^{w_{\rm rx}}(\tau,\nu), \quad (7)$$

where $h_{\rm eff}(\tau,\nu)$ is the effective continuous DD channel (consisting of the cascade of the Tx DD filter, physical DD channel, and Rx DD filter), given by

$$h_{\rm eff}(\tau,\nu) = w_{\rm rx}(\tau,\nu) *_\sigma h(\tau,\nu) *_\sigma w_{\rm tx}(\tau,\nu), \quad (8)$$

and $n_{\rm dd}^{w_{\rm rx}}(\tau,\nu) = w_{\rm rx}(\tau,\nu) *_\sigma n_{\rm dd}(\tau,\nu)$ is the filtered AWGN in DD domain. The DD signal $y_{\rm dd}^{w_{\rm rx}}(\tau,\nu)$ is sampled on the information lattice, resulting in the discrete quasi-periodic DD domain received signal $y_{\rm dd}[k,l]$ as

$$y_{\rm dd}[k,l] = y_{\rm dd}^{w_{\rm rx}}\left(\tau = \frac{k\tau_{\rm p}}{M}, \nu = \frac{l\nu_{\rm p}}{N}\right), \quad k,l \in \mathbb{Z}, \quad (9)$$

which is given by

$$y_{\rm dd}[k,l] = h_{\rm eff}[k,l] *_{\sigma{\rm d}} x_{\rm dd}[k,l] + n_{\rm dd}[k,l], \quad (10)$$

where the $*_{\sigma{\rm d}}$ in (10) is twisted convolution in discrete DD domain, i.e.,

$$h_{\rm eff}[k,l] *_{\sigma{\rm d}} x_{\rm dd}[k,l] = \sum_{k',l'\in\mathbb{Z}} h_{\rm eff}[k-k', l-l']x_{\rm dd}[k',l'] e^{j2\pi\frac{k'(l-l')}{MN}}, \quad (11)$$

where the effective channel filter $h_{\rm eff}[k,l]$ and filtered noise samples $n_{\rm dd}[k,l]$ are given by

$$h_{\rm eff}[k,l] = h_{\rm eff}\left(\tau = \frac{k\tau_p}{M}, \nu = \frac{l\nu_p}{N}\right), \quad (12)$$

$$n_{\rm dd}[k,l] = n_{dd}^{w_{\rm rx}}\left(\tau = \frac{k\tau_p}{M}, \nu = \frac{l\nu_p}{N}\right). \quad (13)$$

Due to the quasi-periodicity in the DD domain, it is sufficient to consider the received samples $y_{\rm dd}[k,l]$ within $\mathcal{D}_0$. The $y_{\rm dd}[k,l]$ samples are written in a vector form and the end-to-end DD I/O relation is written in matrix-vector form as

$$\mathbf{y} = \mathbf{H}_{\rm eff}\mathbf{x} + \mathbf{n}, \tag{14}$$

where $\mathbf{x}, \mathbf{y}, \mathbf{n} \in \mathbb{C}^{MN\times 1}$, such that their $(kN+l+1)^{\rm th}$ entries are given by $x_{kN+l+1} = x_{\rm dd}[k,l]$, $y_{kN+l+1} = y_{\rm dd}[k,l]$, $n_{kN+l+1} = n_{\rm dd}[k,l]$, and $\mathbf{H}_{\rm eff} \in \mathbb{C}^{MN\times MN}$ is the effective channel matrix such that

$$\mathbf{H}_{\rm eff}[k'N+l'+1, kN+l+1] = \sum_{m,n\in\mathbb{Z}} h_{\rm eff}[k'-k-nM, l'-l-mN] e^{j2\pi nl/N} e^{j2\pi \frac{(l'-l-mN)(k+nM)}{MN}}, \tag{15}$$

where $k', k = 0, \cdots, M-1$ and $l', l = 0, \cdots, N-1$.

A. MIMO-Zak-OTFS system model

In this subsection, we extend the SISO Zak-OTFS system model in the above to a MIMO setting as follows. Consider a spatially multiplexed MIMO-Zak-OTFS system with n_t antennas at the transmitter and n_r antennas at the receiver as shown in Fig. 2, with $n_r \geq n_t$. Let $h_{qp}(\tau,\nu)$ denote the impulse response of the channel in DD domain between pth transmitter antenna and qth receiver antenna. Assuming that there are P paths between each pair of transmit and receive antennas, $h_{qp}(\tau,\nu)$ can be written as $h_{qp}(\tau,\nu) = \sum_{i=1}^{P} h_{qpi}\delta(\tau-\tau_{qpi})\delta(\nu-\nu_{qpi})$, where the ith path between the pth transmit antenna and qth receive antenna has delay τ_{qpi}, Doppler ν_{qpi}, and fade coefficient h_{qpi}, where $p = 1, \cdots, n_t$, $q = 1, \cdots, n_r$, and $i = 1, \cdots, P$. The effective channel between pth transmit antenna and qth receive antenna is given by the cascaded twisted convolution operation as follows:

$$h_{{\rm eff},qp}(\tau,\nu) = w_{\rm rx}(\tau,\nu) \ *_\sigma \ h_{qp}(\tau,\nu) \ *_\sigma \ w_{\rm tx}(\tau,\nu). \tag{16}$$

Using (10), the discrete DD domain received signal at the qth receiver antenna is given by

$$y_{{\rm dd},q}[k,l] = \sum_{p=1}^{n_t} h_{{\rm eff},qp}[k,l] \ *_{\sigma{\rm d}} x_{{\rm dd},p}[k,l] + n_{{\rm dd},q}[k,l]. \tag{17}$$

Vectorizing the above relation, we obtain

$$\mathbf{y}_q = \sum_{p=1}^{n_t} \mathbf{H}_{qp} \ \mathbf{x}_p + \mathbf{n}_q, \tag{18}$$

where $\mathbf{y}_q$, $\mathbf{x}_p$ and $\mathbf{n}_q$ are $MN\times 1$ vectors and $\mathbf{H}_{qp}$ is a $MN\times MN$ matrix. Concatenating these received signal vectors, we can write

$$\underbrace{\begin{bmatrix}\mathbf{y}_1\\ \mathbf{y}_2\\ \vdots\\ \mathbf{y}_{n_r}\end{bmatrix}}_{\mathbf{y}_{\rm MIMO}} = \underbrace{\begin{bmatrix}\mathbf{H}_{11} & \mathbf{H}_{12} & \dots & \mathbf{H}_{1n_t}\\ \mathbf{H}_{21} & \mathbf{H}_{22} & \dots & \mathbf{H}_{2n_t}\\ \vdots & \vdots & \ddots & \vdots\\ \mathbf{H}_{n_r1} & \mathbf{H}_{n_r2} & \dots & \mathbf{H}_{n_rn_t}\end{bmatrix}}_{\mathbf{H}_{\rm eff,MIMO}} \underbrace{\begin{bmatrix}\mathbf{x}_1\\ \mathbf{x}_2\\ \vdots\\ \mathbf{x}_{n_t}\end{bmatrix}}_{\mathbf{x}_{\rm MIMO}} + \underbrace{\begin{bmatrix}\mathbf{n}_1\\ \mathbf{n}_2\\ \vdots\\ \mathbf{n}_{n_r}\end{bmatrix}}_{\mathbf{n}_{\rm MIMO}}, \tag{19}$$

resulting in a vectorized I/O relation for MIMO-Zak-OTFS as

$$\mathbf{y}_{\rm MIMO} = \mathbf{H}_{\rm eff,\ MIMO}\ \mathbf{x}_{\rm MIMO} + \mathbf{n}_{\rm MIMO}, \tag{20}$$

where $\mathbf{y}_{\rm MIMO}$, $\mathbf{n}_{\rm MIMO} \in \mathbb{C}^{n_rMN\times 1}$, $\mathbf{x}_{\rm MIMO} \in \mathbb{C}^{n_tMN\times 1}$and $\mathbf{H}_{\rm eff,\ MIMO} \in \mathbb{C}^{n_rMN\times n_tMN}$. Assuming that the receive antennas are to be sufficiently placed apart, the noise vectors at different receive antennas are independent of each other, i.e.,

$$\mathbf{C}_{\mathbf{n}_{\rm MIMO}} = \mathbb{E}\left[\mathbf{n}_{\rm MIMO}\mathbf{n}_{\rm MIMO}^H\right] = \begin{bmatrix}\mathbf{C}_{n_1} & \mathbf{0} & \dots & \mathbf{0}\\ \mathbf{0} & \mathbf{C}_{n_2} & \dots & \mathbf{0}\\ \vdots & \vdots & \ddots & \vdots\\ \mathbf{0} & \mathbf{0} & \dots & \mathbf{C}_{n_r}\end{bmatrix}, \tag{21}$$

where $\mathbf{C}_{n_q} = \mathbb{E}\left[\mathbf{n}_q\mathbf{n}_q^H\right]$ for $q = 1, \cdots, n_r$.

III. Proposed I/O relation estimation and detection for MIMO-Zak-OTFS

The vectorized I/O relation of MIMO-Zak-OTFS in (20) can be used to perform I/O relation estimation and signal detection. In that direction, we propose a I/O relation estimation scheme for MIMO-Zak-OTFS and a low-complexity local search based algorithm for signal detection.

A. I/O relation estimation

In this subsection, we present an I/O relation estimation scheme for MIMO-Zak-OTFS. We use exclusive pilot frames for I/O relation estimation. An exclusive pilot frame is sent every spatial coherence interval. The I/O relation is read off from the received pilot frame. The estimated I/O relation is used for signal detection in data frames sent in the same coherence interval. We illustrate the proposed I/O relation estimation scheme for a MIMO-Zak-OTFS system with $n_t = n_r = 2$ as follows. The pilot symbol is placed at location $(k_{\rm p}, l_{\rm p})$ in the pilot frame. For transmit antenna 1 ($\rm Tx_1$), the pilot symbol is placed at $(k_{\rm p}, l_{\rm p}) = (0,0)$, and for transmit antenna 2 ($\rm Tx_2$), the pilot symbol is placed at $(k_{\rm p}, l_{\rm p}) = (M/2, N/2)$ (see Fig. 3). The pilot frame symbols $x_{{\rm p},1}[k,l]$ and $x_{{\rm p},2}[k,l]$ for $\rm Tx_1$ and $\rm Tx_2$ are given by

$$x_{{\rm p},1}[k,l] = \begin{cases}\sqrt{\frac{E_{\rm p}}{2}}, & (k,l) = (0,0)\\ 0, & \text{otherwise,}\end{cases} \tag{22}$$

$$x_{{\rm p},2}[k,l] = \begin{cases}\sqrt{\frac{E_{\rm p}}{2}}, & (k,l) = \left(\frac{M}{2}, \frac{N}{2}\right)\\ 0, & \text{otherwise.}\end{cases} \tag{23}$$

Normalizing the channel gains to unity and using unit energy DD filters, we get the received average energy at both receiver antennas ($\rm Rx_1$ and $\rm Rx_2$) as $E_{\rm p}$. We obtain the pilot responses $y_{{\rm p},1}[k,l]$ and $y_{{\rm p},2}[k,l]$ in the fundamental region at receiver antennas 1 and 2 ($\rm Rx_1$ and $\rm Rx_2$) respectively. Reading off the green-shaded region in the received pilot frame $y_{{\rm p},1}[k,l]$, denoted by $y_{{\rm p},1}^{(g)}[k,l]$, the effective I/O relation $\hat{h}_{{\rm eff},11}[k,l]$ between $\rm Tx_1$ and $\rm Rx_1$ is estimated as follows:

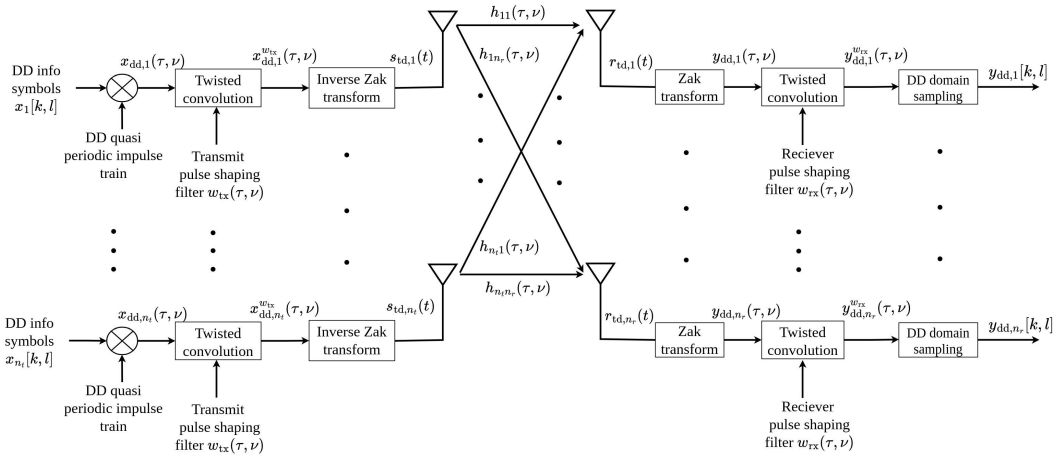

Fig. 2: MIMO-Zak-OTFS modulation scheme.

$$\hat{h}_{\text{eff},11}[k,l] = \begin{cases} y^{(g)}_{\text{p},1}[k,l], & 0 \le k < \frac{M}{2},\ 0 \le l < \frac{N}{2} \\ y^{(g)}_{\text{p},1}[k+M,l]\, e^{-j2\pi\frac{l}{N}}, & -\frac{M}{2} \le k < 0,\ 0 \le l < \frac{N}{2} \\ y^{(g)}_{\text{p},1}[k,l+N], & 0 \le k < \frac{M}{2},\ -\frac{N}{2} \le l < 0 \\ y^{(g)}_{\text{p},1}[k+M,l+N]\, e^{-j2\pi\frac{l}{N}}, & -\frac{M}{2} \le k < 0,\ -\frac{N}{2} \le l < 0 \\ 0, & \text{otherwise,} \end{cases} \quad (24)$$

where

$$y^{(g)}_{\text{p},1}[k,l] = \begin{cases} \sqrt{\frac{2}{E_{\text{p}}}}\, y_{\text{p},1}[k,l], & \left|\frac{k-\frac{M}{2}}{\frac{M}{2}}\right| + \left|\frac{l-\frac{N}{2}}{\frac{N}{2}}\right| > 1 \\ 0, & \text{otherwise} \end{cases}. \quad (25)$$

Likewise, reading off the red-shaded region in the received pilot frame $y_{\text{p},1}[k,l]$, denoted by $y^{(r)}_{\text{p},1}[k,l]$, the effective I/O relation $\hat{h}_{\text{eff},12}[k,l]$ between Tx_2 and Rx_1 is estimated as

$$\hat{h}_{\text{eff},12}[k,l] = \begin{cases} y^{(r)}_{\text{p},1}\left[k+\frac{M}{2}, l+\frac{N}{2}\right] e^{-j\pi\frac{l}{N}}, & -\frac{M}{2} \le k < \frac{M}{2},\ -\frac{N}{2} \le l < \frac{N}{2} \\ 0, & \text{otherwise.} \end{cases} \quad (26)$$

where

$$y^{(r)}_{\text{p},1}[k,l] = \begin{cases} \sqrt{\frac{2}{E_{\text{p}}}}\, y_{\text{p},1}[k,l], & \left|\frac{k-\frac{M}{2}}{\frac{M}{2}}\right| + \left|\frac{l-\frac{N}{2}}{\frac{N}{2}}\right| \le 1, \\ 0, & \text{otherwise.} \end{cases} \quad (27)$$

In a similar way, the estimates $\hat{h}_{\text{eff},21}[k,l]$ and $\hat{h}_{\text{eff},22}[k,l]$ can be obtained by reading off $y^{(g)}_{\text{p},2}[k,l]$ and $y^{(r)}_{\text{p},2}[k,l]$, respectively. Using these discrete DD effective channel estimates, the matrices $\hat{\mathbf{H}}_{11}$, $\hat{\mathbf{H}}_{12}$, $\hat{\mathbf{H}}_{21}$, and $\hat{\mathbf{H}}_{22}$ are constructed using (15). The $\hat{\mathbf{H}}_{\text{eff, MIMO}}$ is obtained by concatenating these matrices as

$$\hat{\mathbf{H}}_{\text{eff, MIMO}} = \begin{bmatrix} \hat{\mathbf{H}}_{11} & \hat{\mathbf{H}}_{12} \\ \hat{\mathbf{H}}_{21} & \hat{\mathbf{H}}_{22} \end{bmatrix}. \quad (28)$$

We note that the proposed way of pilot placement in the transmit frame and choosing the read-off regions in the received frame is aimed at minimizing the interference between the two pilots at the receiver. This approach recovers most of the discrete DD effective channel taps which helps to reduce the estimation error.

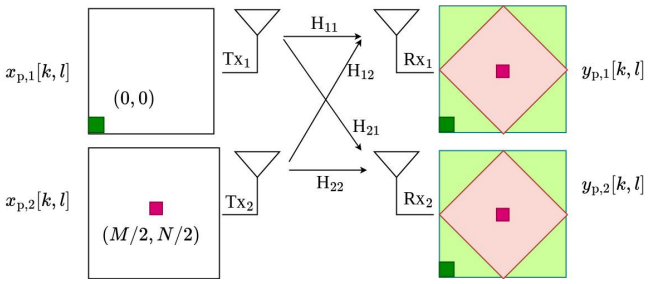

Fig. 3: Pilot placement and read-off region in a 2×2 MIMO-Zak-OTFS system.

B. Signal detection

The estimated $\hat{\mathbf{H}}_{\text{eff, MIMO}}$ matrix in the previous subsection is used for signal detection using (20). As widely considered in the Zak-OTFS literature, we first consider MMSE detection. We also consider a local search based algorithm, namely, likelihood ascent search (LAS) algorithm [16], to achieve improved BER performance. The matrix that minimizes the mean square error $\mathbb{E}\left[\|\mathbf{x}_{\text{MIMO}} - \mathbf{G}\mathbf{y}_{\text{MIMO}}\|^2\right]$ is $\mathbf{G}_{\text{mmse}} = \mathbf{H}^H_{\text{eff,MIMO}}\left(\mathbf{H}_{\text{eff,MIMO}}\mathbf{H}^H_{\text{eff,MIMO}} + \mathbf{C}_{\mathbf{n}_{\text{MIMO}}}\mathbf{I}\right)^{-1}$, and the MMSE detector output vector $\hat{\mathbf{x}}_{\text{MIMO}}$ is obtained as $\hat{\mathbf{x}}_{\text{MIMO}} = f(\mathbf{G}_{\text{mmse}}\mathbf{y}_{\text{MIMO}})$, where $f(.)$ maps each entry of $\mathbf{G}_{\text{mmse}}\mathbf{y}_{\text{MIMO}}$ to a symbol in the modulation alphabet $\mathbb{A}$ based on minimum Euclidean distance.

We improve the MMSE solution vector by performing a local neighborhood search using the LAS algorithm in [16] with MMSE detector output vector as the initial solution vector. The neighborhood is defined as the set of vectors which differ from the current solution vector in one coordinate. If the best neighbor of the current solution vector is better than the current solution vector in terms of maximum-likelihood (ML) cost $\|\mathbf{y}_{\text{MIMO}} - \mathbf{H}_{\text{eff,MIMO}}\mathbf{x}_{\text{MIMO}}\|_2^2$, then that neighbor is taken as the current solution and the algorithm proceeds to the next iteration. The process continues till a local minima is reached, which is declared as the detected vector. We call this detector as the MMSE-LAS detector.

TABLE I: Power-delay profile of Veh-A channel model

Path number (i)	1	2	3	4	5	6
τ_i (μs)	0	0.31	0.71	1.09	1.73	2.51
Relative power (p_i) dB	0	-1	-9	-10	-15	-20

IV. Results and Discussions

In this section, we evaluate the performance of the proposed I/O relation estimation and signal detection schemes in a 2×2 MIMO-Zak-OTFS system with $n_t = n_r = 2$. Simulations are performed for the considered 2×2 MIMO-Zak-OTFS system with the following parameters: Doppler period $\nu_{\rm p} = 15$ kHz, delay period $\tau_{\rm p} = \frac{1}{\nu_{\rm p}} = 66.66$ μs, $M = 12$, $N = 14$, total frame duration $T = N\tau_{\rm p} = 0.93$ ms, bandwidth $B = M\nu_{\rm p} = 180$ kHz, and BPSK. We consider the Vehicular-A channel model [17] with fractional delays and Dopplers, $P = 6$ paths, maximum Doppler $\nu_{\max} = 815$ Hz, maximum delay $\tau_{\max} = 2.51\mu$s, and power delay profile given in Table I. The Doppler associated with the ith path is modeled as $\nu_i = \nu_{\max}\cos(\theta_i)$ where θ_is are independent and uniformly distributed in $[0, 2\pi)$. Sinc, Gaussian, and Gaussian-sinc pulse shaping filters are considered. The sinc filter is given by $w_{\rm tx}(\tau,\nu) = \sqrt{B}{\rm sinc}(B\tau)\sqrt{T}{\rm sinc}(T\nu)$, the Gaussian filter is given by $w_{\rm tx}(\tau,\nu) = \left(\frac{2\alpha_\tau B^2}{\pi}\right)^{\frac{1}{4}} e^{-\alpha_\tau B^2\tau^2} \left(\frac{2\alpha_\nu T^2}{\pi}\right)^{\frac{1}{4}} e^{-\alpha_\nu T^2\nu^2}$, and the Gaussian-sinc filter is given by $w_{\rm tx}(\tau,\nu) = \Omega_\tau\Omega_\nu\sqrt{BT}{\rm sinc}(B\tau){\rm sinc}(T\nu)e^{-\alpha_\tau B^2\tau^2}e^{-\alpha_\nu T^2\nu^2}$. To ensure no bandwidth and time expansion beyond B and T, respectively, $\alpha_\tau = \alpha_\nu = 1.584$ is used for Gaussian filter. Similarly, for Gaussian-sinc filter, $\alpha_\tau = \alpha_\nu = 0.044$ and $\Omega_\tau = \Omega_\nu = 1.0278$ are used. The receive filter at the receiver matched to the transmit filter is given by $w_{\rm rx}(\tau,\nu) = w^*_{\rm tx}(-\tau,-\nu)\ e^{j2\pi\tau\nu}$.

A. MSE performance

Here, we present the performance of the proposed I/O relation estimation scheme in terms of MSE performance. The MSE is defined as MSE $= \frac{\|\mathbf{H}_{\text{eff, MIMO}} - \widehat{\mathbf{H}}_{\text{eff,MIMO}}\|_{\mathbf{F}}^2}{\|\mathbf{H}_{\text{eff, MIMO}}\|_{\mathbf{F}}^2}$. Figure 4 shows the MSE vs pilot SNR performance for the considered 2×2 MIMO-Zak-OTFS system with different filters. From Fig. 4, it is observed that sinc filter gives relatively poor MSE performance compared to Gaussian and Gaussian-sinc filters. This is due to the high sidelobes in the sinc filter, which causes interference. In contrast, Gaussian and Gaussian-sinc filters give better MSE performance, with Gaussian filter performing best. This is because of the very low sidelobes in the Gaussian filter, which provides very good localization of the pulse in the DD domain. The Gaussian-sinc filter has lower sidelobes compared to the sinc filter but higher than the Gaussian filter [15]. Hence, the Gaussian-sinc filter performance is in between those of sinc and Gaussian filters.

B. BER performance

Here, we present the signal detection performance (in terms of BER) achieved by the MMSE and MMSE-LAS detectors in the 2×2 MIMO-Zak-OTFS system for different filters. We present the detection performance for two cases. In the first case, perfect channel state information (CSI), i.e., perfect knowledge of $\mathbf{H}_{\text{eff,MIMO}}$ matrix, is used for detection. In the second case, the estimated $\hat{\mathbf{H}}_{\text{eff,MIMO}}$ matrix obtained using the proposed I/O relation estimation scheme is used for detection.

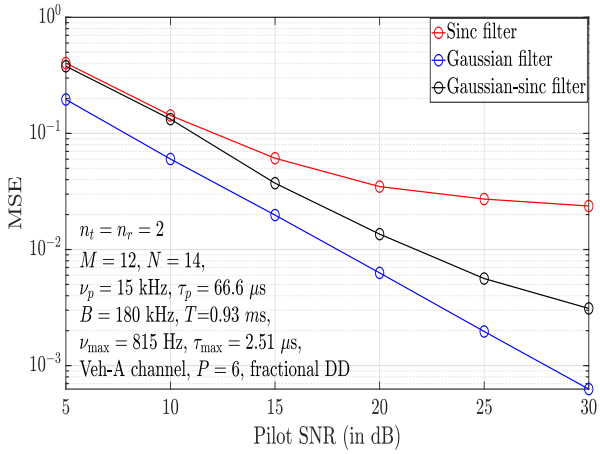

Fig. 4: MSE vs pilot SNR of 2×2 MIMO-Zak-OTFS.

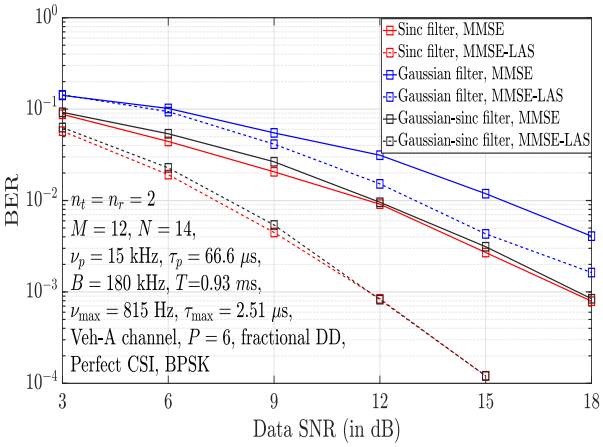

Fig. 5: BER vs data SNR performance of 2×2 MIMO-Zak-OTFS under perfect CSI.

Figure 5 shows the BER performance achieved by the MMSE and MMSE-LAS detectors for sinc, Gaussian, and Gaussian-sinc filters under perfect CSI condition. From Fig. 5, we observe that sinc filter gives better BER performance compared to Gaussian filter. This is because sinc pulse shape has nulls at the DD sampling points, and hence there is no interference at the sampling points. This results in the best detection performance for sinc filter under perfect CSI. The main lobe in Gaussian filter has high non-zero value at the sampling point, which degrades performance. Like sinc filter, the Gaussian-sinc filter also has nulls at the sampling points. This makes its performance very close to that of the sinc filter. Also, MMSE-LAS detection is noted to improve beyond the MMSE detection performance. For example, compared to MMSE detection, MMSE-LAS detection achieves a 6 dB gain in SNR at a BER of 10^{-3} for sinc and Gaussian-sinc filters.

Figure 6 shows the detection performance when the proposed estimated I/O relation is used for detection. The pilot

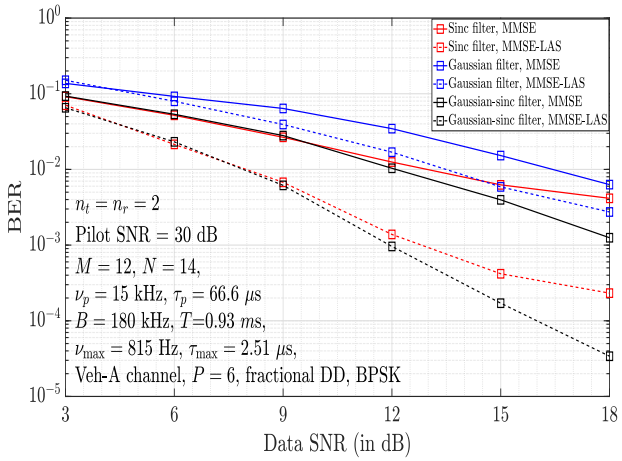

Fig. 6: BER vs data SNR performance of 2×2 MIMO-Zak-OTFS with I/O relation estimation.

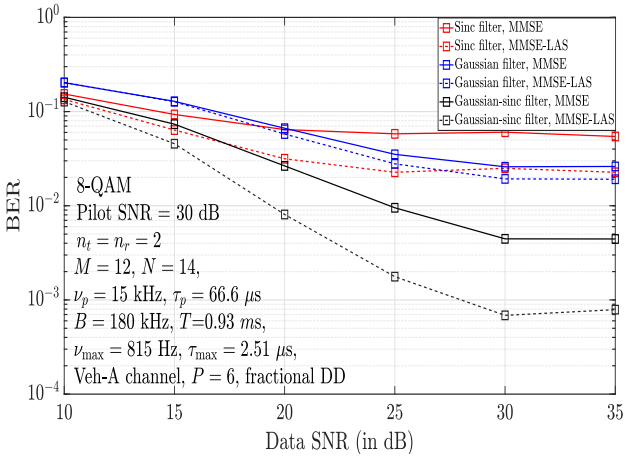

Fig. 7: BER vs data SNR performance of 2×2 MIMO-Zak-OTFS with I/O relation estimation for 8-QAM.

SNR used is 30 dB. We observe that the BER performance for sinc filter is relatively poor in spite of its good main lobe with nulls at sampling points, which can be attributed to its poor estimation performance due to its high side lobes. On the other hand, the BER performance for Gaussian filter is worse than other filters as it has poor main lobe characteristics (high non-zero value at sampling point). Gaussian-sinc filter has both nulls at sampling points as well as low side lobes. This makes its BER performance better than both Gaussian and sinc filters. Also, MMSE-LAS outperforms MMSE because of the the local search in the neighborhood of the MMSE solution.

Figures 5 and 6 show BER performance for BPSK modulation alphabet. Performance for higher-order modulation can also be obtained. Figure 7 illustrates the performance for 8-QAM alphabet. Similar to BPSK, Gaussian-sinc filter gives better performance for 8-QAM as well. Also, MMSE-LAS shows improvement over MMSE detection.

V. Conclusions

We investigated the problem of I/O relation estimation and signal detection in Zak-OTFS receivers in a MIMO setting. We derived the MIMO-Zak-OTFS system model that aids the development of techniques and algorithms for these estimation and detection tasks. We proposed a I/O relation estimation scheme in a model-free framework and devised a pilot placement scheme for the transmit pilot frame and a suitable choice of read-off region in the corresponding received pilot frame at the receiver. The proposed estimation scheme was shown to achieve very good MSE performance for the Gaussian pulse shaping filter. We also improved upon the BER performance of the MMSE detector through the use of a low complexity local search-based algorithm. The Gaussian-sinc filter was shown to achieve good BER performance with the proposed I/O relation estimation and signal detection schemes. MIMO-Zak-OTFS with embedded and superimposed pilot frames where both pilot and data symbols co-exist in a given frame can be taken up for future work.

References

[1] R. Hadani *et al.*, "Orthogonal time frequency space modulation," *Proc. IEEE WCNC'2017*, pp. 1-6, Mar. 2017.

[2] R. Hadani and A. Monk, "OTFS: a new generation of modulation addressing the challenges of 5G," available online: arXiv:1802.02623v1 [cs.IT] 7 Feb 2018.

[3] P. Raviteja, K. T. Phan, Y. Hong, and E. Viterbo, "Interference cancellation and iterative detection for orthogonal time frequency space modulation," *IEEE Trans. Wireless Commun.*, vol. 17, no. 10, pp. 6501-6515, Oct. 2018.

[4] M. K. Ramachandran and A. Chockalingam, "MIMO-OTFS in high-Doppler fading channels: signal detection and channel estimation," *Proc. IEEE GLOBECOM'2025*, pp. 206-212, Dec. 2018.

[5] Best Readings in Orthogonal Time Frequency Space (OTFS) and Delay Doppler Signal Processing, https://www.comsoc.org/publications/best-readings/orthogonal-time-frequency-space-otfs-and-delay-doppler-signal-processing.

[6] S. K. Mohammed, R. Hadani, A. Chockalingam, and R. Calderbank, "OTFS — a mathematical foundation for communication and radar sensing in the delay-Doppler domain," *IEEE BITS the Inform. Theory Mag.*, vol. 2, no. 2, pp. 36-55, 1 Nov. 2022.

[7] S. K. Mohammed, R. Hadani, A. Chockalingam, and R. Calderbank, "OTFS — predictability in the delay-Doppler domain and its value to communication and radar sensing," *IEEE BITS the Inform. Theory Mag.*, vol. 3, no. 2, pp. 7-31, Jun. 2023.

[8] S. K. Mohammed, R. Hadani, and A. Chockalingam, *OTFS Modulation – Theory and Applications*, IEEE press-Wiley, Nov. 2024.

[9] S. Gopalam, I. B. Collings, S. V. Hanly, H. Inaltekin, S. R. B. Pillai, and P. Whiting, "Zak-OTFS implementation via time and frequency windowing," *IEEE Trans. Commun.*, vol. 72, no. 7, pp. 3873-3889, Jul. 2024.

[10] S. Gopalam, H. Inaltekin, I. B. Collings, and S. V. Hanly, "Optimal Zak-OTFS receiver and its relation to the radar matched filter," *IEEE Open J. of the Commun. Soc.*, vol. 5, pp. 4462-4482, 2024.

[11] M. Ubadah, S. K. Mohammed, R. Hadani, S. Kons, A. Chockalingam, and R. Calderbank, "Zak-OTFS for integration of sensing and communication," available online: arxiv:2404.04182v1 [eess.SP] 5 Apr 2024.

[12] J. Jayachandran, R. K. Jaiswal, S. K. Mohammed, R. Hadani, A. Chockalingam, and R. Calderbank, "Zak-OTFS: pulse shaping and the tradeoff between time/bandwidth expansion and predictability," available online: arxiv:2405.02718v1 [eess.SP] 4 May 2024.

[13] B. Dabak, V. Khammammetti, S. K. Mohammed, and R. Calderbank, "Zak-OTFS and LDPC codes," *Proc. IEEE ICC'2024*, pp. 3785-3790, Jun. 2024.

[14] F. Jesbin and A. Chockalingam, "Near-optimal detection of Zak-OTFS signals," *Proc. IEEE ICC'2024*, pp. 4476-4481, Jun. 2024.

[15] A. Das, F. Jesbin, and A. Chockalingam, "A Gaussian-sinc pulse shaping filter for Zak-OTFS," online arXiv:2502.03904v1 [cs.IT] 6 Feb 2025.

[16] A. Chockalingam and B. Sundar Rajan, *Large MIMO Systems*, Cambridge University Press, 2014.

[17] ITU-R M.1225,"Guidelines for evaluation of radio transmission technologies for IMT-2000," *International Telecommunication Union Radio communication*, 1997.